6. THE OPERATIONAL ORBIT

Planned to be operated in geostationary orbit by means of a single ground station, the satellite was actually operated from a highly elliptical (geostationary transfer) orbit. The parameters of the actual orbit are given, along with a summary of the features of the elliptical orbit which complicated the satellite operations and performances: the resulting radiation environment (considered in more detail in Chapter 7), eclipses (affecting the power budget), Earth and Moon occultations (affecting the observation programme), and the complex ground-station requirements—a single ground station would have resulted in a maximum of 30 per cent of useful data collection, and additional ground stations had to be rapidly brought into the telecommunication network. The problems affecting the satellite attitude control—perturbing torques especially those around perigee, and the consequences on the real-time attitude determination, and the (general) problem of micrometeoroid impacts—are discussed.

6.1. Orbital Elements

The orbital characteristics for the epoch 18 September 1989, when the revised mission manoeuvres had been completed, were as follows:

- perigee height: 526 km
- apogee height: 35 900 km
- orbital period: 640 min
- eccentricity: 0.72
- inclination: 6°.8
- ascending node: 105°
- argument of perigee: 214°

The observed evolution of some of these parameters during the mission is shown in Figure 6.1 and Figure 6.2. Additional information on the orbit evolution can be found in Volume 3, Chapter 8.

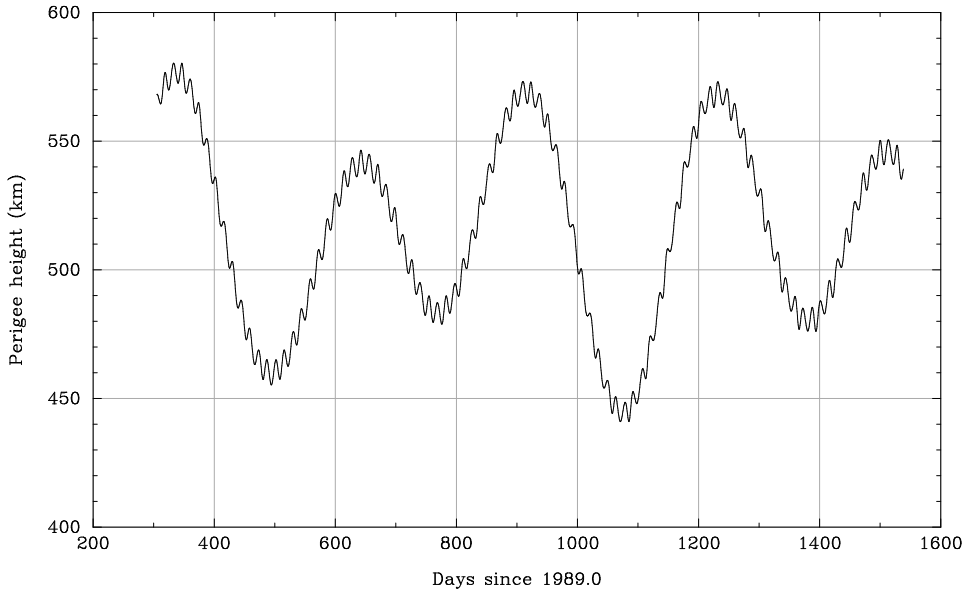

Figure 6.1. *Evolution of perigee height during the mission.*

For Hipparcos, a critical assessment of the accuracy and precision of the orbit data was essential. Preliminary analysis of the orbit determination accuracy assumed a perigee altitude of 600 km and three ranging stations. The covariance analysis showed that the semi-major axis could be determined to better than 10 m and the inclination to about $0\overset{\circ}{.}001$. The positional and velocity accuracy would vary along the orbit, as shown in Table 6.1. These data compared well with the orbit determination accuracy at that time:

- perigee/apogee altitude: ±150 m
- semi-major axis: ±50 m
- inclination: $\pm 0\overset{\circ}{.}2$
- apogee position: ±1.5 km
- apogee velocity: ±0.08 m s^{-1}

Specifications for the revised orbit included an instantaneous knowledge of the position to 1.5 km (in order to be able to account for positional observations of solar system objects), and the velocity to 0.2 m s^{-1} (in order to be able to correct for aberration). These criteria were achieved by the adopted ranging and orbital reconstruction procedures.

The orbit data, which included the time interval, the state vector components at a given reference time in the mean equinox of date frame, auxiliary Keplerian motion parameters, and Chebychev expansion of each of the six state components, was sent to the data reduction teams with the telemetry data.

Table 6.1. Variation in the position and velocity accuracy along the orbit.

Time since perigee (hours)	Position accuracy (km)	Velocity accuracy (m/s)
0.0	0.87	0.78
0.5	0.70	0.32
1.0	0.79	0.18
2.0	1.03	0.11
3.0	1.20	0.07
4.0	1.28	0.06
5.0	1.30	0.06

6.2. Radiation Environment

The revised orbit meant that the satellite was subject to a much higher particle radiation exposure than anticipated prior to launch. Consequently, radiation damage to the solar arrays and other payload and spacecraft equipment was higher than had been anticipated. In particular, the increased radiation led to the progressive degradation of the solar arrays, difficulties in maintaining the on-board attitude control and the failure of the satellite gyros. Details of the associated problems are presented in more detail in Chapters 7, 11, and 15.

6.3. Eclipses

In geostationary transfer orbit between zero and six eclipses due to the Moon occurred annually, with an average of three. The duration of these eclipses ranged from a few minutes to over four hours. Long eclipses occurred at the Sun-Moon-apogee-Earth conjunction. Eclipses by the Earth occurred about four times per day, with a duration range of a few minutes to more than one hour. Long eclipses occurred at a Sun-Earth-apogee conjunction. The duration of the eclipses are illustrated in Figure 4.1.

The distribution of eclipse durations are tabulated in Table 6.2. During its lifetime the critical eclipses for Hipparcos were March 1989 (eclipse duration 104 min), April 1993 (63 min) and August 1993 (82 min).

Coupled with the solar panel degradation problem was the fact that, in the elliptical orbit, the eclipses of the Sun by the Earth were much longer (up to 100 min) and much more frequent than in the geostationary case. During eclipses, the spacecraft could only function by extracting power from its batteries. Thus the power deficit problem was enhanced during the period of the longest eclipses and had to be solved with more drastic measures. Detailed power budgets and the relevant operational procedures were prepared to ‘hibernate’ the spacecraft in such cases when the batteries could not supply enough energy to maintain a fully nominal mission throughout the eclipse.

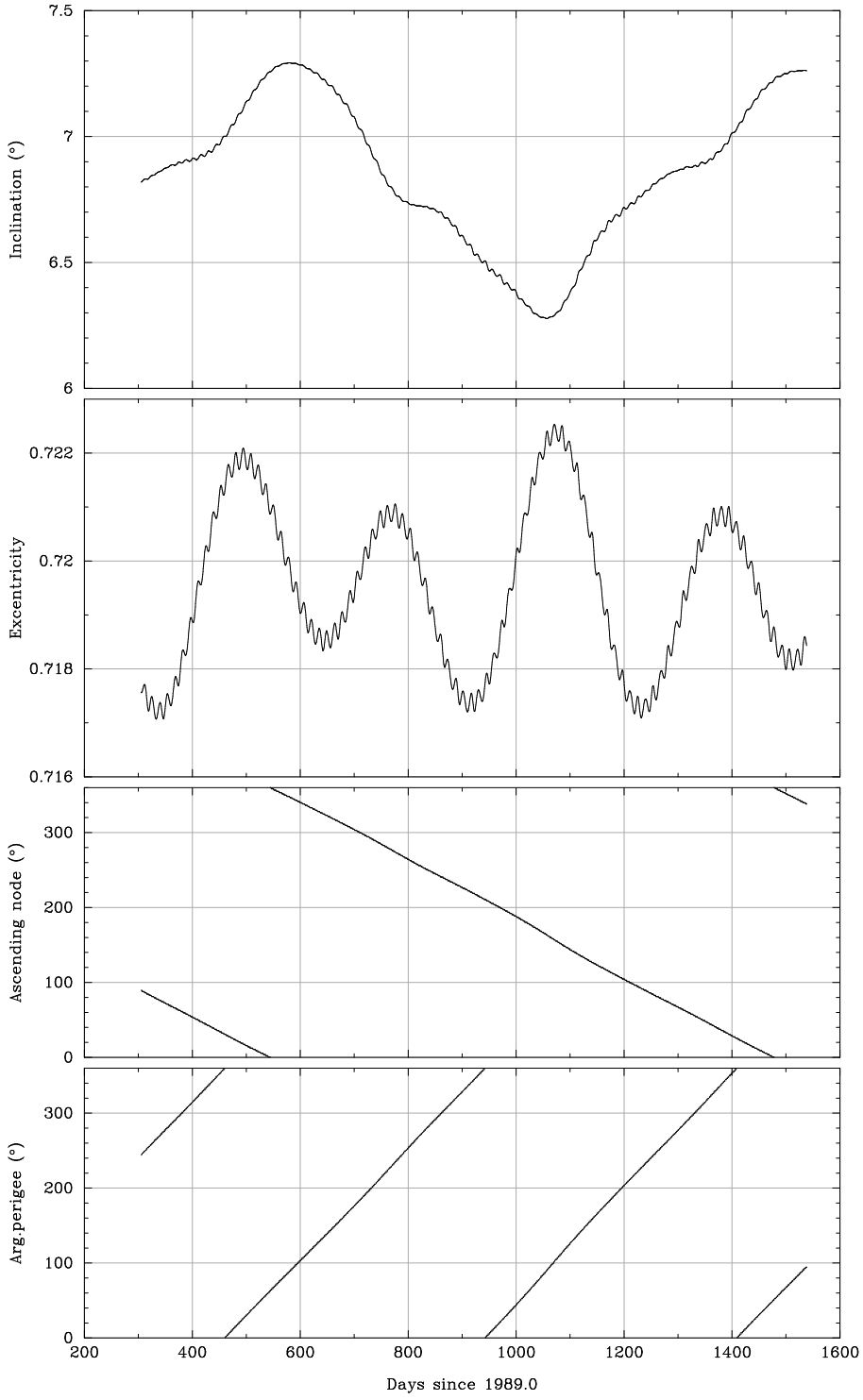

Figure 6.2. *Evolution of inclination, eccentricity, and angle during the mission.*

Table 6.2. Distribution of eclipse durations for a three-year mission in geostationary transfer orbit (approximately 2500 orbits).

Eclipse duration	%
0 to 20 min	18
20 to 30 min	44
30 to 60 min	26
over 60 min	12

In order to survive the long eclipse period (up to 104 min), a power saving strategy was developed, which guaranteed a positive power budget by decreasing or switching off loads. As a reference criterion the remaining time between end of charge of the batteries and the start of the next eclipse was taken. This time was calculated and extrapolated in real-time to ensure immediate implementation of the relevant power saving procedures. However, no such drastic measures were actually needed up to 30 March 1993, since even at the longest eclipse times the batteries were always fully charged before the next eclipse entry.

6.4. Occultations

Occultations occurred when one of the two fields of view crossed the Earth or the Moon. The payload detectors would have been damaged by these events, if they had not been shielded by shutters which closed at these times. The Earth occultations, like the eclipses, occurred more frequently and lasted longer in the elliptical than in the geostationary orbit, again reducing the amount and uniform time coverage of good science data. Also, when they occurred near perigee, they increased the risk of loss of attitude control by blinding the star mapper.

6.5. Ground Station Coverage

One of the most serious operational consequences of being in a geostationary transfer type orbit is that one ground station is not sufficient to track the satellite at all times. At the beginning of the mission, complete operational support was only available for about one third of the time, posing major problems on how to manage the mission outside visibility periods. The major problems to be solved were how to keep real-time attitude determination convergence until the next visibility period and how to protect the spacecraft, with appropriate reconfigurations of the subsystems, against such events as eclipses, occultations, perigee passages and possible on-board failures.

As described in Chapter 4 the number of ground stations was quickly increased to three. However, the lowest part of the orbit was only rarely trackable, and in any case only from Kourou (near the equator).

6.6. Perturbing Torques

In geostationary orbit, the only significant external disturbance torques acting on the spacecraft were expected to be due to the solar radiation pressure and the constantly spinning gyros. However, away from apogee of the revised orbit, other effects became significant, e.g. atmospheric, magnetic dipole and gravity gradient torques all played a role depending on the altitude and attitude of the satellite. Their combined effect degraded the on-board attitude control to the extent that ground support was often required. In addition, greatly increased cold gas consumption was necessary to control the attitude through these variable conditions, implying a shorter lifetime, based only on consumables. The higher torques also degraded the on-ground attitude determination.

6.7. Loss of Real-Time Attitude Determination

The difficulties involved in controlling the spacecraft attitude in the revised mission, arose from the critical link between the stellar measurements, the attitude measurements made on-board, and the attitude control. The approximate positions of all stars to be observed by the main detector were uplinked to the satellite in the form of expected times at which the stars were predicted to cross the star mapper slit measurement system, based on the nominal attitude of the satellite. The actual star transits across the star mapper slit system were detected and converted into actual crossing times. These times allowed the on-board computer to calculate the difference between the nominal and actual satellite attitude for a subset of the brighter programme stars.

Radiation from the van Allen belts blinded the photomultiplier which sampled the star mapper data: the on-board processor was then not able to filter out a star transit from the noise. At such times, the spacecraft was without external references and had to rely on the gyros alone for real-time attitude determination, except for increasingly refined modelling carried out towards the end of the mission allowing attitude control in the absence of one or more gyros (see Chapters 14–16). Close to perigee, the external disturbance torques were greatest, causing long thruster firings approximately once per minute. Studies later in the mission suggested that the gyro drifts also evolved more quickly around perigee. Both phenomena combined to cause a drift of the spacecraft without correction from the star mapper.

When the real-time attitude determination estimate differed by more than 10 arcsec from the actual spacecraft attitude, ground intervention was required to increase tolerances to the maximum value of 30 arcsec. If the real-time attitude determination estimate differed by more than 30 arcsec, further intervention was required using ground software to re-initialise real-time attitude determination. The resulting effects are described in more detail in Chapters 13 and 14.

6.8. Micrometeoroids

A potential hazard faced by satellite experiments is the impact of micrometeoroids. Although no specific events were ever attributed to micrometeoroid impacts on the Hipparcos satellite, a careful evaluation was made of the expected effects in advance of launch, both in order to assess possible attitude perturbations caused by impacts with the more common, lighter particles, and the risk of catastrophic damage by the rarer but more massive particles. In view of its applicability to other missions, a summary of the predicted effects are therefore given hereafter.

A dust experiment on HEOS-2 provided much data on the micrometeoroid environment in near-Earth orbit. The data could be categorised into three groups according to the observed rate. Event rates of 1 or more events per 15 min were classified as swarms, between 1 event per 15 min and 2 events per day was considered a group, and fewer than 2 events per day was attributed to random particles. Analysis of the event rates indicated that the apex particles (where the apex is the direction of the Earth's velocity around the Sun) were most frequent. Their average impact velocity was around 10 km s^{-1} resulting in a flux of $\phi_{\text{apex}} = 4 \times 10^{-4}$ m^{-2} s^{-1} $(2\pi \text{ sr})^{-1}$ for masses $\geq 10^{-12}$ g. The 'ecliptic-south particles', although almost as frequent as the apex particles, were much smaller and faster giving a correspondingly lower flux. These latter particles are believed to be fragmentation products from larger micrometeoroids.

An important result from the HEOS-2 experiment was that more than 80 per cent of all the detected particles arrived in swarms or groups. The groups showed a correlation with the Moon position suggesting a lunar origin—these particles may be ejected from the Moon's surface by impacting meteorites in the kg range. The swarms were found mainly in the near-Earth part of the orbit, and showed no lunar correlation prompting suggestions that they may be produced by meteors impinging on the Earth's atmosphere.

Simulations of the Effect of Micrometeoroids on Hipparcos

Simulations based on published data (Naumann, 1966) were undertaken before launch to assess the effect of micrometeoroid impacts on Hipparcos in orbit. The simulations were constructed as follows: (i) the satellite was hit by a random sized meteoroid at times which were uniformly distributed within the interval 0 to 10 000 s; (ii) the meteoroid velocity (v) was uniformly distributed in the range ± 47 km s^{-1}; (iii) each impact reached a target point on one of the solar panels at r = 1.8 m from the centre of the satellite and hits on the satellite body were neglected; (iv) the number of hits was calculated from the flux data as twice the product of the cumulative flux (for particles heavier than 1×10^{-15} kg), the total area of the solar panels (6.8 m^2) and the integration time. The factor of two arose from allowing both forward and backward hits; (v) the cumulative flux (given in impacts per m^2) of Landolt-Börnstein (1981) was used:

$$\phi = 5 \times 10^{-5} \left(\frac{m}{10^{-15}} \right)^{-0.4} \quad \text{for} \quad m < 1.4 \times 10^{-10} \text{ kg} \qquad [6.1]$$

$$\phi = 2 \times 10^{-1} \left(\frac{m}{10^{-15}} \right)^{-1.1} \quad \text{for} \quad m > 1.4 \times 10^{-10} \text{ kg}$$

This gave a change in angular momentum per hit of $\delta L = mvr$, and a change in angular velocity of $\delta\omega = \delta L / I$, where a mean value ($I = 400$ kg m^2) of the satellite's moment of inertia was used.

In this way successive impacts gave positive or negative increments of the angular velocity. In each time interval between hits, the velocity increment was integrated up to a change in angle. The nominal rotation of the satellite and the smooth perturbations due to solar radiation pressure were not included, so that the results only represent the additional effects caused by micrometeoroids.

The cumulative flux was also used to predict the masses of the impacting meteoroids. The data can be represented by the relation:

$$\left(\frac{m}{m_0}\right)^a = \frac{\phi}{\phi_0} = R \qquad [6.2]$$

where m_0 is the smallest mass considered, ϕ_0 is the flux of particles with $m > m_0$ and a is a negative constant. Two different values of a were used: $a = -0.4$ for m $< 1.4 \times 10^{-10}$ kg and $a = -1.1$ for higher masses (see Equation 6.1). Masses consistent with the flux data could be generated according to the formula:

$$m = m_0 R^{a^{-1}} \qquad [6.3]$$

when R is uniformly distributed between 0 and 1. To increase the number of data points, angle values were linearly interpolated between impact times such that one data point was obtained for every 10 s of the 10 000 s interval. A cubic spline was then fit with a knot every 100 s and the difference between the data and the spline function was then calculated. The residuals of this fit were taken as a measure of the micrometeoroid effect. A total of 1000 simulations of 10 000 s were made.

The results showed that the most frequent residual lay around 1×10^{-5} arcsec which was a factor of 10^{-3} smaller than the expected accuracy of the individual measurements made by the Hipparcos instruments. Only a few of the 1000 simulations had rms residuals in the vicinity of 10^{-2} and the median rms effect was 2.6×10^{-6} arcsec. In 2.5 years the simulations predicted about 500 impacts resulting in residuals $> 10^{-2}$ arcsec. The single largest impact during that period was predicted to produce residuals of the order of 10 arcsec.

The following analysis of the micrometeoroid problem also yielded similar results. Taking particles with mass $m = 10^{-12}$ g as representative, a satellite moment of inertia, $I = 350$ kg m^2, $v = 30$ km s^{-1} and an impact distance of $d = 1$ m from the center of mass yielded: $\delta\omega = mvd / I = 10^{-8}$ arcsec s^{-1}, with an average occurrence of about 1 event per 100 s. At the extreme end of the mass range (see Figure 6.3) particles of mass 10^{-3} g would give an increment to the spin velocity of approximately 10 arcsec s^{-1} about once per year.

The conclusion of these studies was that it was unlikely that most micrometeoroid impacts would have any major effects on the accuracy of the Hipparcos observations, but that larger, more infrequent events could significantly perturb the satellite attitude. In reality, it was difficult to ascribe any evolution of the satellite attitude unambiguously to the effects of micrometeoroids, and they certainly resulted in no evident threat or degradation of the mission performances.

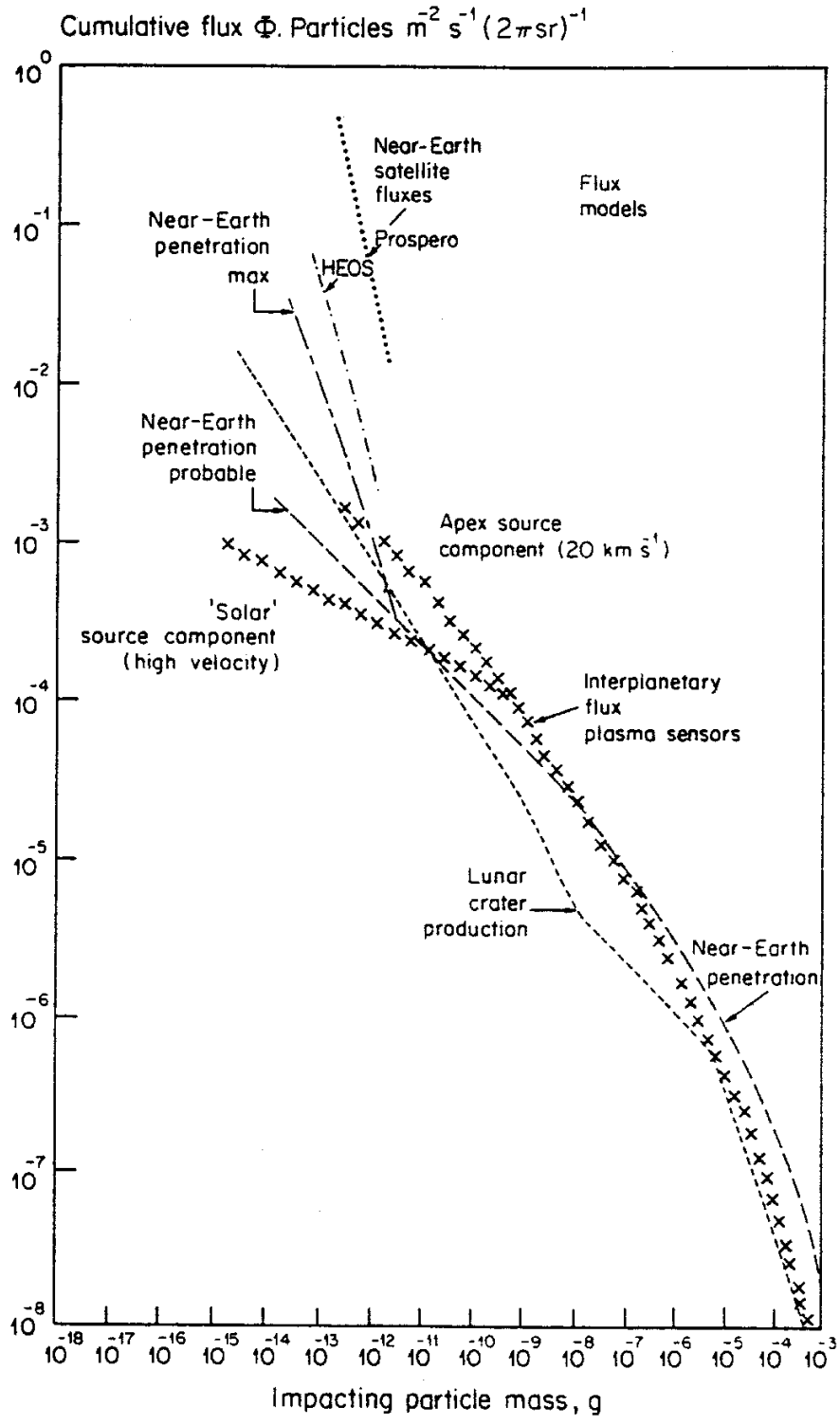

Figure 6.3. *Inter-comparison of models of the cumulative particle flux derived from near-Earth satellites, interplanetary probes and lunar flux measurements (from Cosmic Dust, J.A.M. McDonnell, 1978).*

The 1993 Perseid Meteoroid Shower

Although the Hipparcos mission was terminated before the 1993 Perseid shower, a careful evaluation of its potential effect was made, since periodic, seasonally correlated enhancements of meteoroid flux towards the Earth are quite normal, and are associated with trails of dust material along cometary orbits which the Earth crosses at fixed times of the year. The given maxima are very stable in terms of epoch, but they may increase considerably if the Earth crosses the path of the comet shortly after the comet itself.

As simulations had shown, the impact of meteoroid showers on the Hipparcos satellite during its mission were in general expected to be almost negligible. An exception to this might have been the 12 August 1993 Perseid shower, which was predicted to be unusually strong as a result of the perihelion passage of the Perseid's source comet, Swift-Tuttle, the previous year (31 December 1992). This expectation was based on analogy with the largest known meteor storm prior to this, the 17 November 1966 Leonid storm. Both the Leonids and the Perseids are of cometary origin, the former being associated with comet Temple-Tuttle with a period of 33.25 years, the latter with comet Swift-Tuttle with period 130 years. Prior to the storm of November 1966 there was a steady increase in Leonid meteoroid activity, a pattern also seen in the tenfold increase in Perseid activity in the previous two years. Less than one year prior to the Leonid storm the source comet passed its perihelion. The Perseid's source comet, Swift-Tuttle, passed its perihelion less than one year prior to expected storm activity.

At the time of the 1966 Leonid storm the Earth was within 450 000 km of the comet's orbital plane. During the Perseid storm the Earth would be within 140 000 km of the comet's orbital plane. The increase in meteoroid flux, above the mean background, for the Leonid 1966 storm was more than a factor of 1000. The increased Perseid activity was expected to be even greater than this. In particular the flux enhancement with respect to the average meteoroid background flux was expected to be of the order of 1000 or more (it has been shown that during periods of meteor storm activity, the impact probability increases by more than 10^4 over the sporadic background of meteoroids; see Beech, Brown & Jones, 1995). This would imply approximately 0.5 hits m^{-2} hr^{-1} by meteoroids of diameter larger than 0.1 mm on an exposed satellite surface. The impact velocity was expected to be of the order of 60 km s^{-1}, giving an equivalent penetration depth in Al of 5 to 10 times the diameter of the projectile. A 1 mm projectile could cause substantial damage, and even smaller particles of 0.1 mm diameter could disable sensitive spacecraft components such as the solar arrays.

Given the potential risk to the spacecraft and its components from the 1993 Perseid shower, ESOC carried out an assessment of the flux geometry for the predicted time of the Perseid storm relative to the spacecraft. The spin-axis of Hipparcos pointed towards the Sun and thus only the smaller side of the satellite (3.5 m^2) could be targeted by the meteoroids. The configuration between the meteoroids stream and the Sun indicated that the Perseid storm would not be dangerous to Hipparcos. Since the solar arrays were oriented towards the Sun, the solar arrays and the meteoroid stream were almost in the same plane (i.e. the Sun direction was $\alpha = 142°$, $\delta = 15°$, and the Perseid stream was $\alpha = 46°$, $\delta = 58°$). The angle between the two directions was about 80°.5 and thus the angle of impact would be about 9°.5 from the rear of the solar arrays, giving a reduction in the projected surface area of a factor of 6. On this basis it was considered that the overall risk to the spacecraft from this exceptional Perseid storm was not unduly alarming.